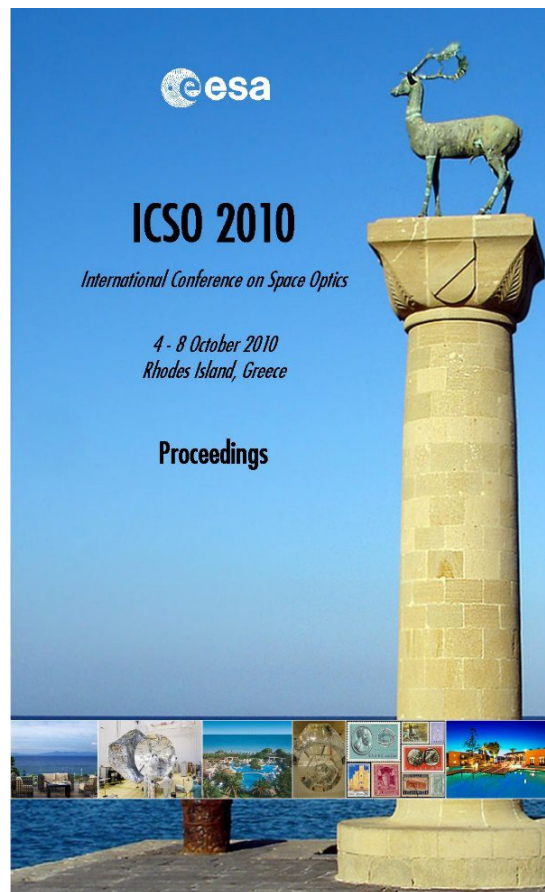# International Conference on Space Optics—ICSO 2010

Rhodes Island, Greece

4–8 October 2010

Edited by Errico Armandillo, Bruno Cugny,
and Nikos Karafolas

Space active optics: in flight aberrations correction for the next generation of large space telescopes

M. Laslandes, M. Ferrari, E. Hugot, G. Lemaitre

SPACE ACTIVE OPTICS: IN FLIGHT ABERRATIONS CORRECTION FOR THE NEXT GENERATION OF LARGE SPACE TELESCOPES

M. Laslandes, M. Ferrari, E. Hugot, G. Lemaitre
Laboratoire d'Astrophysique de Marseille (CNRS and Université de Provence)
38 rue F. Joliot Curie – 13388 Marseille cedex 13 - France
marie.laslandes@oamp.fr

I. INTRODUCTION

The need for both high quality images and light structures is a constant concern in the conception of space telescopes. In this paper, we present an active optics system as a way to fulfill those two objectives. Indeed, active optics consists in controlling mirrors' deformations in order to improve the images quality [1]. The two main applications of active optics techniques are the in-situ compensation of phase errors in a wave front by using a corrector deformable mirror [2] and the manufacturing of aspherical mirrors by stress polishing or by in-situ stressing [3]. We will focus here on the wave-front correction. Indeed, the next generation of space telescopes will have lightweight primary mirrors; in consequence, they will be sensitive to the environment variations, inducing optical aberrations in the instrument.

An active optics system is principally composed of a deformable mirror, a wave front sensor, a set of actuators deforming the mirror and control/command electronics. It is used to correct the wave-front errors due to the optical design, the manufacturing imperfections, the large lightweight primary mirrors' deflection in field gravity, the fixation devices, and the mirrors and structures' thermal distortions due to the local turbulence [4]. Active optics is based on the elasticity theory [5]; forces and/or load are used to deform a mirror. Like in adaptive optics, actuators can simply be placed under the optical surface [1,2], but other configurations have also been studied: a system's simplification, inducing a minimization of the number of actuators can be achieved by working on the mirror design [5]. For instance, in the so called Vase form Multimode Deformable Mirror [6], forces are applied on an external ring clamped on the pupil. With this method, there is no local effect due to the application of forces on the mirror's back face. Furthermore, the number of actuators needed to warp the mirror does not depend on the pupil size; it is a fully scalable configuration.

The insertion of a Vase form Multimode Deformable Mirror on the design of an optical instrument will allow correcting the most common low spatial frequency aberrations. This concept could be applied in a space telescope. A Finite Element Analysis of the developed model has been conducted in order to characterize the system's behavior and to validate the concept.

II. VASE FORM MULTI-MODE DEFORMABLE MIRROR

A. Needs in Space

A Vase form Multi-mode Deformable Mirror (VMDM), as proposed by Lemaitre [6], could be used in the optical train of a space telescope to compensate the deformations of a large, lightweight primary mirror. We can spot the two main reasons making the primary mirror losing its best shape [4]:

- The mirror's thermal dilatations due to the variation of the temperature seen by the telescope, depending on its orbite.

- The weightlessness conditions which will induce a difference in the optical configuration compared with the integration on Earth.

These two causes induce an Optical Path Difference (OPD) in the instrument corresponding to the first classical optical aberrations, corrigible by a VMDM. Following previous studies in close collaboration with the French space agency (CNES) and space industry, we can assume that correcting the first 9 optical modes Spherical3, Coma3, Astigmatism3&5, Trefoil5&7 and Tetrafoil7&9 is enough to significantly improve the wave-front quality. The rms amplitude of the wave-front to be corrected is chosen on the order of $\lambda = 632.8$ nm with a required precision of $\lambda/20$ rms in Wave-Front for each mode.

The design of the correcting mirror for such an application has also to consider some particular constraints such as the weight, the volume, the power consumption or the resistance to the launch vibrations [7].

B. Principle of deformation and design

A VMDM has the following geometry:

- A meniscus corresponding to a circular plate of radius a and thickness t_1

- An outer ring at the edge of the meniscus, its radius is b and its thickness $t_2 > t_1$

- k_m clamped arms, regularly distributed along the outer ring, going from the radius b to a radius c, their thickness is t_3

The deformation of the mirror's pupil is obtained by applying a set of $2k_m$ discrete forces, $F_{a,k}$ and $F_{c,k}$, located on the ring (at $r = a$) and at the end of each arm (at $r = c$).

The behavior of such a mirror corresponds to small deformations of a constant thickness circular plate, and can be described by the elasticity theory [6,8]. In polar coordinates, the equation of a plate deformation, w, is:

$$\nabla^2 \nabla^2 w(r, \theta) = 0 \quad \text{with} \quad D = \frac{Et^3}{12(1-v^2)} \quad , \tag{1}$$

D is the rigidity depending on the thickness of the plates but also on its material via the Young's modulus, E, and the Poisson's ratio, v.

As demonstrated by Lemaitre in Reference 7, the flexure of the meniscus corresponds to the optical modes verifying the condition on the radial and azimuthal order given in Equation (3):

$$w = \sum w_{nm} = \sum A_{nm} r^n \cos(m\theta) \quad , \tag{2}$$

$$\text{with} \quad n = m \quad \text{or} \quad n = m + 2 \quad . \tag{3}$$

So, such a system can compensate a set of Zernike polynomials [9]. Given the symmetry of the modes needed to be generated to meet our specifications, we have chosen to use a mirror with 12 arms, allowing creating the deformations in several orientations. Furthermore, in order to correct the spherical aberration, a central clamping on the back face of the mirror, fixed at its base, is added relatively to the usual VMDM design (Fig. 1).
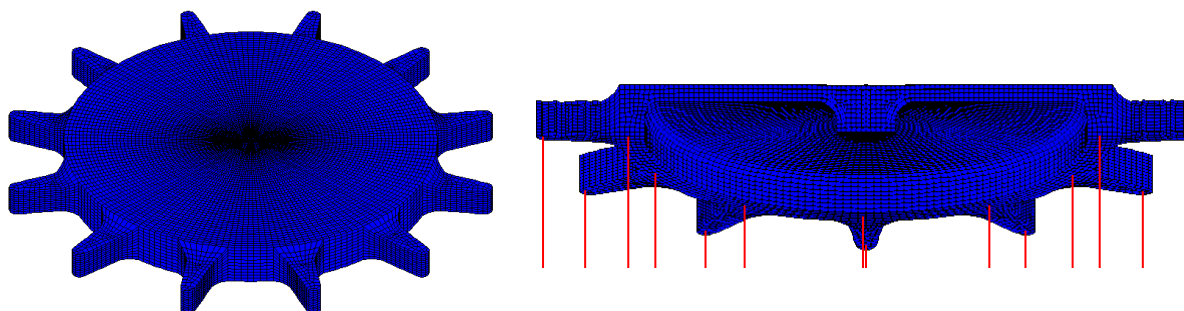
Fig. 1. Finite Elements model of the studied VMDM (77879 nodes, 63708 hexaedrical elements)

In order to have a light system, the dimensions of the studied mirror have been reduced to a minimum. We take the diameter of the group mirror/ring at 100 mm, with a 90 mm diameter optical aperture, and the diameter of the equipped mirror (including the arms) is set to 130 mm. The deformations are produced by applying a displacement on actuators located on the ring and arms. With the described design, we can create an OPD allowing us to compensate the eight optical aberrations presented in the previous section but also any linear combinations of those modes.

All the mirror's characteristics have been optimized to obtain the most efficient system possible. For that purpose, a Finite Element Analysis (FEA) has been performed. In the next section we present the method used to characterize the system.

III. CORRECTING SYSTEM PERFORMANCES

A. Influence Functions and Eigen Modes

Finite Element Analysis (FEA) allows characterizing the mirror's behavior in an accurate way; it takes in account effects such as the fixation device, the boundary conditions or the small geometrical details [10].

Leaning on a VMDM's FEA model (Fig. 1), we develop a method to determine the needed forces using the phase decomposition on the mirror's influence functions base [11,12]. The influence function of an actuator, φ_i^{IF}, is the resulting mirror surface shape when that actuator is given a unit command. This technique, fairly used in adaptive optics, needed to be validated for a different kind of actuators disposition, like on the VMDM design. The differences here are that the actuators, used to produce displacements and slopes, are located around the mirror and generate deformations far from their action points. For a VMDM configuration, there are two types of influence functions: the deformation maps when we push the end of the arm, and when we push on the ring (see Fig. 2.).
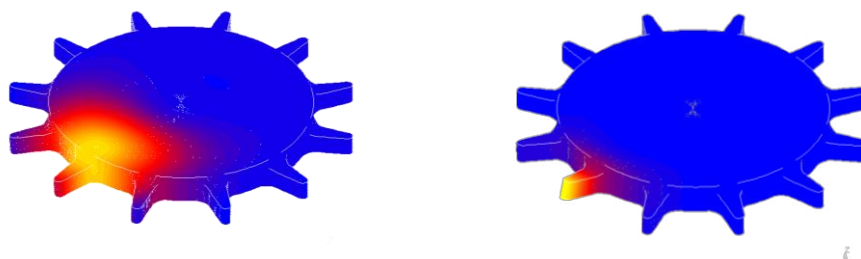

Fig. 2. Influence functions for an actuator in $r = a$ (left) and in $r = c$ (right)

Moreover, the influence functions base gives access to the system's eigen modes. They are shown in Figure 3. They are very close to optical aberrations and represent an orthogonal base of the system: linear combinations of them give all the deformations that the system is able to produce. The modes are classified from the less to the more energetic [12].
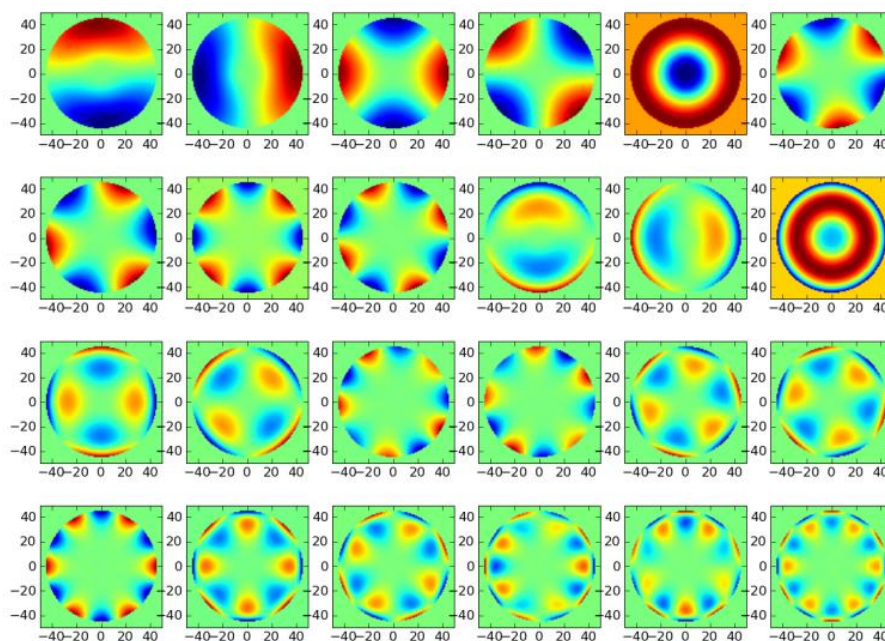

Fig. 3. System eigen modes

The decomposition on the mirror's influence functions or eigen modes allows characterizing the mirror in a fast and accurate way. In the FEA model, we acquire the $2k_m$ influence functions. The decomposition of a phase map on this characteristic base permits to reconstruct the deformation that the system is able to generate. Comparing it to the initial phase, the precision of the correction is determined (see Fig. 4).
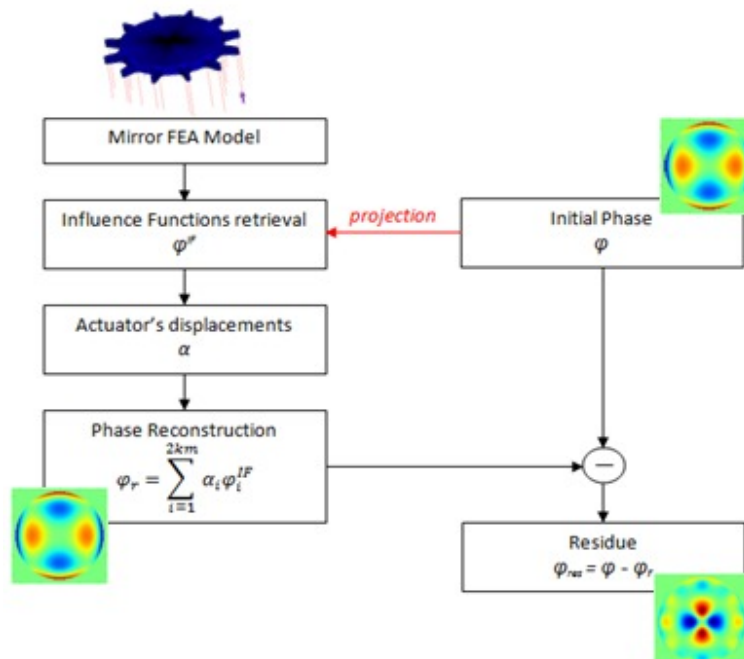
Fig. 4. Method to characterize the VMDM performances

B. Modes correction

The purity of each mode is determined by calculating the residues obtained when the aberration is corrected with an amplitude of λ. The results are presented on the left of Figure 5. With less than 2% of residues, the Coma3, Trefoil5 and Astigmatism3 are precisely corrected (WFE < $\lambda/60$ rms). Trefoil7, Tetrafoil7 can be generated with 5% of residues and they are just at the $\lambda/20$ specification. On the other hand, the amount of residues for Astigmatism5 is just above the specification and the Spherical3 and Tetrafoil9 aberrations induce more residues (around $\lambda/8$). We can note that residues mainly come from the presence of the central clamping and from the difference between the modes' symmetry and the mirror symmetry.
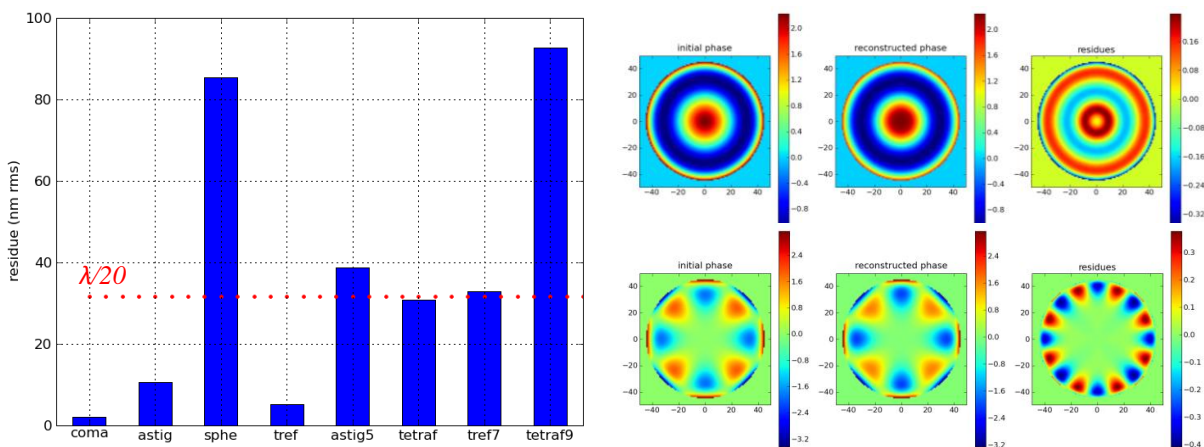

Fig. 5. Left: Residue rms for a modal correction of 1λ in WF
Right: Residues location for the Spherical3 (up) and Tetrafoil9 (down) aberrations
(left: initial phase – center: reconstructed phase – right: residues map) – units: mm

On Figure 5 right, we can see the initial phase, the reconstructed phase after decomposition and the residues map for two problematic modes (Spherical3 and Tetrafoil9). The residues' projection on the Zernike polynomials base shows that they are composed of harmonics of the considered aberration.

The mirror having 12 arms, it is also able to correct the Pentafoil and Hexafoil modes but we can see in Figure 3 that they are placed at the end of the table; it means that they require a lot of energy to be obtained. Moreover,

because of their symmetries, the creation of the Pentafoil9 and 11 implies a significant amount of residue. On the contrary, with a residual error of less than 10nm rms, the generation of Hexafoil11 and 13 are really pure. As the Hexafoils can only be generated in one fixed direction, the mirror will have to be oriented if we want to correct this mode.

The projection on the influence functions base gives the values of displacement to be applied in order to generate the given phase. Applying those values in the FEA model we can visualize the mirror deformation (Fig. 6). This last step allows us to validate the decomposition method and to study the system behavior (displacements, stress in the material etc.).
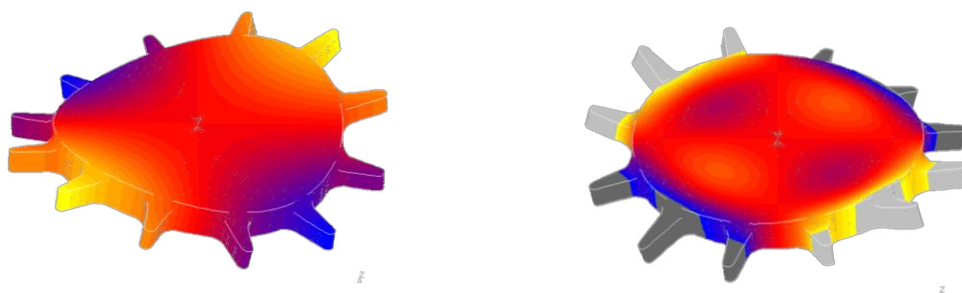

Fig. 6. Mirror deformations corresponding to Astigmatism 3 and 5

C. Wave-front correction

It is important to study the mirror's performances in a situation close to the real functioning of this correcting system. In such a case, the wave-front to be corrected will be a combination of the 8 modes presented before plus others minors terms.

Because the generation of Spherical3 and Tetrafoil9 induces a too much residues, we decide to correct them only up to an amplitude of $\lambda/3$, so that the amount of residue is lower than $\lambda/20$ for each mode.

Firstly, we consider the worst case: the incident phase is composed of the 8 aberrations at their maximum amplitude ($\lambda/3$ rms for Spherical3 and Tetrafoil9, λ rms for Coma3, Astigmatism3&5, Trefoil5&7 and Tetrafoil7). The residual error will be the quadratic sum of each mode's residues. In this configuration, the precision of correction is about $\lambda/8$ rms. Even if it is the worst case, the residual error is quite low.

To have a representative idea of what the system can achieve, we calculate the residual phase after the correction of a random phase map. The optical path difference map is created by adding all the modes, balancing them with a random coefficient between 0 and their maximum corrigible amplitude. Studying the statistics after several random draws (Fig. 7) gives the expected mean precision achievable by the system. For 1000 random maps, the mean precision correction achieved is around $\lambda/15$ rms (red line in Fig. 7) with a standard deviation of $\lambda/60$ (blue lines).
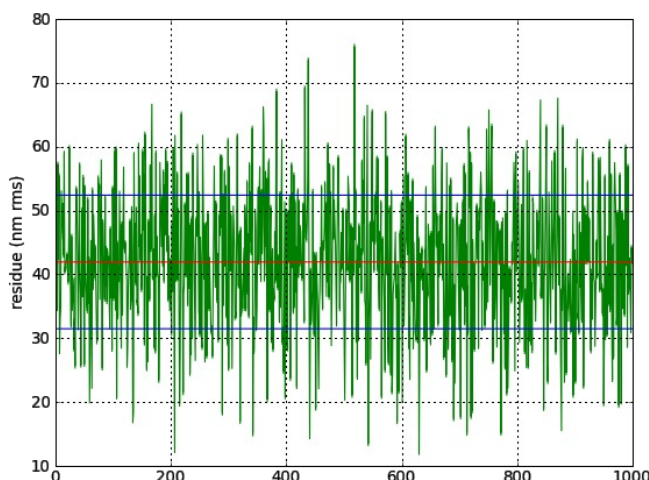

Fig. 7. Residues for the wave-front corrections of 1000 random phase maps

The studied correcting mirror allows achieving a precise correction; indeed, all the modes are generated individually with a residual error smaller than $\lambda/20$ rms and the residues on the total wave-front are expected to be around $\lambda/15$ rms.

IV. CONCLUSIONS

The very simple concept of Multimode Deformable Mirror seems to be applicable and very efficient to improve the wave-front quality in a space telescope. We have seen in this paper that it allows correcting, with a good quality, the first Zernike polynomials: Comas, Astigmatisms, Trefoils and Tetrafoils. The spherical aberration can also be generated with the presence of a central clamping on the mirror's back face. In addition, this holds the entire system. A system with 12 arms is preferred because it can easily create shapes of several symmetries. To characterize the system, we have considered the mirror's influence functions and eigen modes. Knowing these characteristics, the correction capabilities have been determined for each mode separately and for more representative phases. With this work, we have defined some specifications for the amplitudes that can be corrected in an efficient way.

The Comas3, Astigmatisms3&5, Trefoils5&7 and Terafoils7 are easily generated at amplitudes around 1λ rms with a precision better than $\lambda/20$ rms. The corrections of Spherical3 and Tetrafoils9 require more energy and are less precise; we choose to correct them at a maximal amplitude of $\lambda/3$ rms to obtain the same precision. The element inducing a significant part of the residues is the central clamping, but it allows the generation of Spherical3 despite the absence of an uniform load. Simulating the correction of random phase maps, the mean residual phase should be around $\lambda/15$ rms.

Those results are promising for the application of such a concept to the compensation of the deformations in a large space telescope. The next step is to realize a prototype of this correcting mirror and test it in a representative configuration in order to improve the TLR at a level of 4.

REFERENCES

[1] Freeman, R., Pearson, J., "Deformable Mirrors for all Seasons and Reasons", Applied Optics, Vol. 21, No. 4, 1982
[2] Wilson, R., Franza, F., Noethe, L., "Active Optics – I. A System for Optimizing the Optical Quality and Reducing the Costs of Large Telescopes", Journal of Modern Optics, Vol. 34, No.4, 1987
[3] Hugot, E. et al, "Active Optics: Stress Polishing of Toric Mirrors for the VLT SPHERE Adaptive Optics System", Applied Optics, Vol. 48, No. 15, 2009
[4] Kendrew, S., "Lightweight Deformable Mirrors for Ground- and Space-Based Imaging Systems", PhD Thesis, 2006
[5] Lemaitre, G. *"Astronomical Optics and Elasticity Theory – Active Optics Methods",* Springer, 2009
[6] Lemaitre, G., "Active Optics: Vase or Meniscus Multimode Deformable Mirrors and Degenerated Monomode Configurations", Meccanica 40, 233-249, 2005
 [7] CNES, *"Techniques & Technologies des Véhicules Spatiaux"*, Cours de Technologie Spatiale – Volume 1, 1998
[8] Timoshenko, S., Woinowsky-Krieger, S., *"Theory of Plates and Shells"*, McGraw-Hill International Editions, 2nd edition, 1959
[9] Noll, R., "Zernike Polynomials and Atmospheric Turbulence", Optical Society of America, Vol. 66, No. 3, 1976
 [10] Hugot, E., "Optique Astronomique et Elasticité – L'Optique Active dans la Perspective des Télescopes Géants et de l'Instrumentation du Futur", PhD thesis, 2007
[11] Gray, T., "Minimizing High Spatial Frequency Residual in Active Space Telescope Mirrors", PhD Thesis, 2008
[12] Paterson, C., Munro, I., Dainty, J.C., "A Low Cost Adaptive Optics System Using a Membrane Mirror", Optics Express 175, Vol. 6, No. 9, 2000